



No detectable effect of CO₂ on elemental stoichiometry of *Emiliana huxleyi* in nutrient-limited, acclimated continuous cultures

Anja Engel^{1,2,3,*}, Carolina Cisternas Novoa³, Mascha Wurst², Sonja Endres^{1,2},
Tiantian Tang^{3,4}, Markus Schartau¹, Cindy Lee³

¹GEOMAR Helmholtz Centre for Ocean Research, 24105 Kiel, Germany

²Alfred Wegener Institute for Polar and Marine Research (AWI), 27570 Bremerhaven, Germany

³Marine Sciences Research Center, School of Marine and Atmospheric Sciences, Stony Brook University, Stony Brook, New York 11794, USA

⁴Present address: Department of Earth and Planetary Sciences, Harvard University, Cambridge, Massachusetts 02138, USA

ABSTRACT: Effects of CO₂ concentration on elemental composition of the coccolithophore *Emiliana huxleyi* were studied in phosphorus-limited, continuous cultures that were acclimated to experimental conditions for 30 d prior to the first sampling. We determined phytoplankton and bacterial cell numbers, nutrients, particulate components like organic carbon (POC), inorganic carbon (PIC), nitrogen (PN), organic phosphorus (POP), transparent exopolymer particles (TEP), as well as dissolved organic carbon (DOC) and nitrogen (DON), in addition to carbonate system parameters at CO₂ levels of 180, 380 and 750 μ atm. No significant difference between treatments was observed for any of the measured variables during repeated sampling over a 14 d period. We considered several factors that might lead to these results, i.e. light, nutrients, carbon overconsumption and transient versus steady-state growth. We suggest that the absence of a clear CO₂ effect during this study does not necessarily imply the absence of an effect in nature. Instead, the sensitivity of the cell towards environmental stressors such as CO₂ may vary depending on whether growth conditions are transient or sufficiently stable to allow for optimal allocation of energy and resources. We tested this idea on previously published data sets where PIC and POC divided by the corresponding cell abundance of *E. huxleyi* at various *p*CO₂ levels and growth rates were available.

KEY WORDS: Acidification · Cocolithophores · Element composition · Nutrient limitation · Chemostats

Resale or republication not permitted without written consent of the publisher

INTRODUCTION

Large-scale changes in surface ocean chemical equilibrium and in elemental cycling are occurring due to ocean acidification (e.g. Chen & Millero 1979, Brewer et al. 1997, Kleypas et al. 2006). The ocean provides the largest sink for anthropogenic carbon dioxide (CO₂) globally (Sabine et al. 2004). As the inventory of dissolved inorganic carbon (DIC) of the

surface ocean increases due to enhanced uptake of CO₂ from the atmosphere, the pH of seawater decreases. CO₂-related changes in carbonate chemistry of the ocean affect marine biota, and thus the cycling of biogenic elements (Wolf-Gladrow et al. 1999, Beardall & Raven 2004). The biological pump, i.e. the sequestration of biologically fixed carbon from surface waters to below the thermocline, sustains a vertical DIC gradient in the ocean that pro-

motes the uptake of CO_2 from the atmosphere. Because of the vast spatial dimensions of the oceanic system, even small changes in the biological pump could significantly affect atmospheric CO_2 concentration. It has been proposed that calcifying organisms, such as corals, coccolithophores, foraminifera, and pteropods, may particularly suffer from increasing seawater acidification (decreasing pH), because more metabolic energy is required for cellular precipitation of calcium carbonate, which impairs production of mineral shells as well as population growth (Feely et al. 2004).

Many studies of the effect of changing CO_2 on phytoplankton have shown variations in growth, primary production, calcification, the efficiency and regulation of carbon concentration mechanisms, and the production of extracellular organic matter, while others found little or no response (reviewed in Ridgwell et al. 2009, Riebesell & Tortell 2011). Many of these studies use *Emiliania huxleyi* (or a similar coccolithophore) as a model species due to its considerable role in the global carbon cycle and its demonstrated sensitivity to changing $p\text{CO}_2$ (Paasche 2001, Thierstein & Young 2004). Formation of particulate inorganic carbon (PIC) during calcification releases CO_2 , whereas particulate organic carbon (POC) and dissolved organic carbon (DOC) formation during photosynthesis uses CO_2 . The balance between primary production and calcification is therefore an important ratio to measure whether coccolithophores in the ocean act as a net source or sink of CO_2 . The [PIC]:[POC] 'rain' ratio has gathered much attention in studies of the response of coccolithophores to global change, as the ratio of PIC and POC removal from the surface ocean determines CO_2 sequestration on longer time scales. POC concentration in phytoplankton cultures or in the field includes organic carbon in living cells, cell detritus and extracellular particles, such as gel particles. A major class of gel particles is the transparent exopolymer particles (TEP) that form from dissolved polysaccharide precursors by physical coagulation (Engel et al. 2004a).

Acidic polysaccharides originate mainly from phytoplankton exudation, a process that is viewed as a carbon 'overflow' for photosynthesis products under nutrient depletion (e.g. Obernosterer & Herndl 1995, Biddanda & Benner 1997, Søndergaard et al. 2000). As photosynthesis rates increase with CO_2 concentration (Rost et al. 2003), the exudation rate of acidic polysaccharide and therefore TEP production may also rise (Engel 2002). Recent experimental studies indicate that TEP formation increases in response to ocean acidification (Engel 2002, Mari

2008, Engel et al. 2014) and may alter [POC]:[PN] ratios (where PN is particulate nitrogen) during coccolithophore blooms (Engel et al. 2005). Changes in [PIC]:[POC] ratio can be dependent on several factors; the ratio does not automatically reflect changes in the relative amount of precipitated calcium carbonate but can vary solely with carbon quota and TEP concentration.

In contrast to organic matter production, the functionality of calcification in coccolithophores is not well understood. In addition to carbonate chemistry, the calcification rate in *E. huxleyi* is affected by light, salinity, macro- and micronutrient availability, and temperature, and varies with growth rate (Fernández et al. 1996). Indeed, nutrient limitation (particularly phosphorus) has been shown to increase calcification rates relative to photosynthesis, but can also result in formation of malformed or incomplete coccoliths (Paasche 1998, Kaffes et al. 2010). Variations in external growth factors are difficult to control simultaneously under experimental conditions because cell growth itself changes, e.g. nutrient and light availability and therefore growth rate. This challenges the experimental isolation of a single, direct effect of $p\text{CO}_2$ on calcification. Strong co-variations of factors that modify calcification rates must be expected during bloom-like situations, either in the field or during fertilized mesocosm experiments. Even in batch culture experiments, there are problems in continuously tracing nutrient availability and growth rates with time. Different variations in environmental factors thus may partly be responsible for the complex, and in some regard even contrary, picture of the sensitivity of *E. huxleyi* to ocean acidification drawn in previous studies. Increasing $p\text{CO}_2$ was found to either decrease (Riebesell et al. 2000a, Rost et al. 2003, Sciandra et al. 2003a, Zondervan et al. 2002) or increase (Iglesias-Rodriguez et al. 2008a) the concentration of biogenic calcite produced, or to cause no, or a complex, response (Langer et al. 2006, 2009a, De Bodt et al. 2010a). Response to CO_2 of *E. huxleyi* may also involve changes in growth rate (Jones et al. 2013) and may be strain-specific (Raven & Crawford 2012). Apart from multiple changes of growth factors occurring in batch cultures, another general challenge of experimental perturbation studies typically is their short duration (days to weeks), which inevitably bears the risk that observed responses may be transient rather than sustained. Recently, it has been suggested that *E. huxleyi* can adapt to high CO_2 and restore calcification rates within a period of 1 yr, relative to cells grown at present day $p\text{CO}_2$ (Lohbeck et al. 2012). Strain selection and adaptation

may further impact calcification response of natural populations.

A sustained exposure of microorganisms to environmental factors like CO₂ or pH, while keeping other growth factors more stable, can be realized in chemostats. Chemostats are continuous culture systems, in which cell abundance is controlled by the nutrient concentration of the inflow media, while growth rate μ (d⁻¹) is in balance with the rate of the flow (d⁻¹) (Novick & Szilard 1950). During steady state, the growth rate equals the flow rate, and cell abundances remain constant over time. Thus, chemostats enable studies of cell physiology and element composition under constant nutrient-limited growth. Few chemostat experiments with phytoplankton at different *p*CO₂ have been conducted previously (Sciandra et al. 2003a, Leonardos & Geider 2005, Borchard et al. 2011, Borchard & Engel 2012). Interestingly, these studies often showed the largest response to CO₂ during transient phases, i.e. either when transitioning from low to high *p*CO₂ (Sciandra et al. 2003a, Leonardos & Geider 2005) or during the initial transition from the batch to the dilution phase (Borchard et al. 2011).

In the experiments described below, we use nutrient-limited, continuous cultures of *Emiliana huxleyi* to disentangle potential effects of *p*CO₂ from those that are caused by variation in growth rate, as well as by other environmental control factors that impact phytoplankton cell numbers, elemental composition (e.g. PIC:POC), and DOC and TEP concentrations. It has been suggested that calcification rates in coccolithophores are affected by the calcite saturation state (Ω -Ca), and strongly decline at a value of Ω -Ca < 2 (Gehlen et al. 2007). Due to high cell abundance, growth and calcification in coccolithophore cultures may reduce Ω -Ca of the seawater medium to values < 2 (de Bodt et al. 2008), or even cause undersaturation during low dilution rates in chemostats (Borchard et al. 2011). Ocean acidification will likely cause a decline in CaCO₃ saturation state; however, Ω -Ca values in surface waters will be > 2 in most parts of the future ocean. During this study, we therefore followed the suggestions of LaRoche et al. (2010) to circumvent strong declines in Ω -Ca by increasing alkalinity in the initial medium reservoir. Cultures were acclimated to the different *p*CO₂ values for about 1 mo when steady state growth was reached and cell abundances were comparable between different chemostats; this minimized transient responses. Thus, our experiment aimed at studying sustained responses in element composition of *E. huxleyi* to realistic changes in *p*CO₂ and Ω -Ca, while reducing variations in environmental co-factors.

MATERIALS AND METHODS

To separate potential effects of *p*CO₂ from other environmental factors, we conducted a chemostat experiment with constant cell growth rate, temperature and nutrient supply, while CO₂ aeration was varied to achieve partial pressures of 180, 380 and 750 μ atm.

We used the calcifying strain of *Emiliana huxleyi* (PML B92/11A) because it had responded to changes in *p*CO₂ during previous batch experiments (Riebesell et al. 2000a, Zondervan et al. 2002). As mentioned above, cells were acclimated over a period of 1 mo prior to the first sampling to avoid short-term stress effects on cell composition. Sampling was repeated 5 times during steady-state growth over a period of 14 d to assure the reproducibility of results. We chose a low flow rate of media (0.2 d⁻¹) because *E. huxleyi* often occurs in nutrient-limited areas (Tyrrell & Taylor 1996, Lessard et al. 2005) where low growth rates prevail. In addition to the particulate elements POC, PIC, PN and POP, we sampled for DOC and TEP to ascertain the role of gel particle formation in POC production.

Experimental set-up. A total of 5 chemostats (60 cm height \times 15 cm diameter) with culture volumes of 9.2 l each were used during this study. The chemostat and its associated components are described in detail in Borchard et al. (2011). Desired CO₂ concentrations of 180, 380 (duplicate chemostats) and 750 μ atm (duplicate chemostats) were achieved by continuous aeration with CO₂ gas. CO₂ parameters were measured as also described in Borchard et al. (2011). Experiments were conducted at 14°C under P-limitation (N:P of 30:1) and at 190 μ E m⁻² s⁻¹; 16:8 light:dark. Although light intensity and light/dark cycle can be adjusted individually for each chemostat (TL-D DeluxPro, Philips; QSL 100) in our system, the same light conditions were provided for each chemostat culture during this study. Light was measured with a light sensor (Biospherical Instruments) in the air above the seawater inside the chemostats.

Preparation of *E. huxleyi* culture and addition to chemostats followed the description in Borchard et al. (2011). Culture medium for the experiment was prepared from 0.2 μ m filtered natural North Sea seawater with a salinity of 33, pH of 8.20 and total alkalinity (TA) of 2250 μ mol kg⁻¹, and enriched with macronutrients to yield final concentrations of 43 μ M NO₃⁻ and 1.5 μ M PO₄³⁻ to favor phosphorus limiting conditions, as P limitation can initiate blooms of *E. huxleyi* in the field (Aksnes & Egge 1991, Aksnes et al. 1994). Draw-down of carbonates in a coccolitho-

phore culture reduces alkalinity of seawater, and can strongly affect seawater pH or even cause carbonate undersaturation that could impact calcification in *E. huxleyi* (Borchard et al. 2011). To minimize effects of calcification by *E. huxleyi* on carbonate chemistry in the incubators, TA in the reservoir tank was increased by addition of bicarbonate to $2460 \mu\text{mol kg}^{-1}$ (LaRoche et al. 2010).

Target temperature and $p\text{CO}_2$ were established in incubators within 2 d prior to cell addition. *E. huxleyi* cells were inoculated into each chemostat to a final density of $5000 \text{ cells ml}^{-1}$, and grown in batch mode for 5 d. Afterwards, flow was started and then continued for 38 d at a dilution rate (D) of 0.2 d^{-1} . Gentle mixing of the culture at 50 rpm was applied to keep cells in suspension. Steady state in a chemostat is reached when biomass (or cell abundance) remains constant over time, as the dilution rate equals the growth rate (μ), and was established on Day 28 of this experiment (Fig. 1).

Distinct $p\text{CO}_2$ concentrations in the chemostat cultures were achieved using a CO_2 regulation system consisting of commercially available mass flow controllers (Type 1179 Mass Flo Controller; MKS Instruments) and a pressure vessel. Target CO_2 concentrations are reached by 2-step-down regulation of pure CO_2 (CO_2 4.5; $\geq 99.995 \text{ vol } \%$; Air Liquide) to the target CO_2 level using CO_2 -free air (domnick hunter CO_2 scrubber $\text{CO}_2\text{RP}280$; accuracy $< 1 \mu\text{atm}$). CO_2 concentrations in the air/ CO_2 mixture of the inflow were determined before and after the experiment using an infrared CO_2 analyzer (LI-COR, 6252). Pre-

vious evaluation of the system showed high precision and stability of air flows with variations of $< 2 \%$ (Borchard et al. 2011). For continuous evaluation of the system, pH and temperature inside each chemostat were recorded hourly over the whole duration of the experiment.

All pipes and tubes were acid rinsed (10% HCl) and sterilized by autoclaving (121°C for 30 min). All non-autoclavable parts, e.g. incubator and reservoir vessels, were cleaned with phosphate-free detergent, soaked in 10% HCl for 2 h and then thoroughly rinsed with deionized water.

Total alkalinity (TA). TA in 25 ml samples was measured by titrating with 0.05 M HCl until the buffering capacity of the water samples was consumed and all bases of interest were protonated to zero level species. Analysis was accomplished with an automatic titrator (TitroLine® alpha plus, SI Analytics) equipped with a sample changer (TW alpha plus, SI Analytics) and a piston burette (Titronic®110 plus, SI Analytics). The concentration of TA ($\mu\text{mol kg}^{-1}$ seawater) was calculated from linear regression of the absolute numbers of protons in solution and the total volume (sample plus HCl) in the range of pH 3 to 4.

pH and temperature. pH and temperature values were recorded every hour on a data logger throughout the entire experiment using WTW pH 340i handheld meters and WTW standard DIN/NBS buffers (PL 4, PL 7 and PL 9) recalibrated using Tris based reference material provided by A. Dickson (pers. comm.). Accuracy of measurement was better than ± 0.005 pH and $\pm 0.1^\circ\text{C}$ for temperature.

$p\text{CO}_2$, and calcite saturation state

($\Omega\text{-Ca}$). The full carbonate system speciation and $\Omega\text{-Ca}$ in chemostat cultures and medium reservoirs were calculated from pH and TA values at each sampling time with the CO_2sys program (Lewis & Wallace 1998), using the carbonic acid dissociation constants of Mehrbach et al. (1973) refitted by Dickson & Millero (1987), and the HSO_4^- dissociation constant of Dickson et al. (1990) on the US National Bureau of Standards scale. The saturation state ($\Omega\text{-Ca} = [\text{Ca}^{2+}][\text{CO}_3^{2-}]/K_{\text{sp}}$) of calcite was computed using the calcite solubility (K_{sp}) of Mucci (1983).

***E. huxleyi* abundance.** *E. huxleyi* cell numbers in all chemostats were measured daily, but samples for all

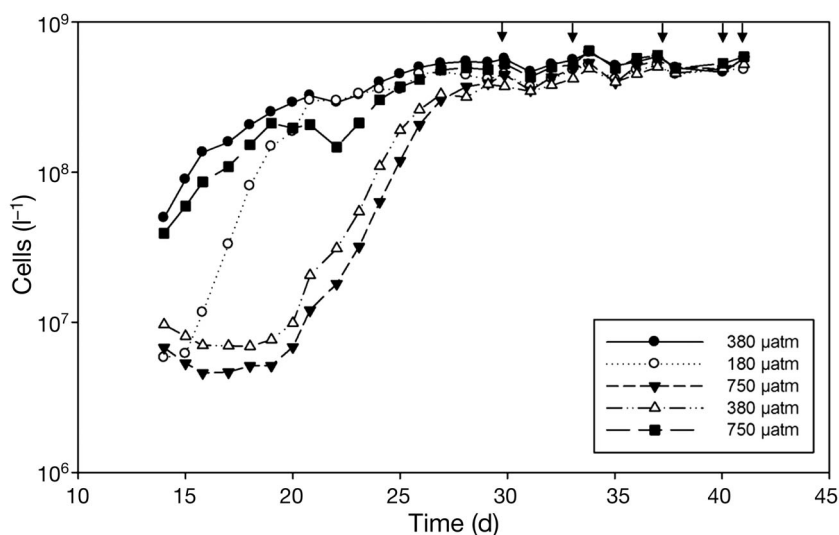


Fig. 1. Number of *Emiliana huxleyi* cells (l^{-1}) over time during continuous flow in the chemostats as well as sampling times during the steady-state phases (arrows). Duplicate chemostats were run at $380 \mu\text{atm}$ and $750 \mu\text{atm}$ CO_2 , while a single chemostat was run at $180 \mu\text{atm}$ CO_2

other parameters were regularly taken only after steady state was reached, i.e. on Days 30, 34, 38, 42, and 44 of the experiment (Fig. 1). Samples were always taken at the same time of the day (3 h after lights on). Cell abundance and volume were determined in triplicate using a Beckman Coulter MultiSizer III. Particles with an equivalent spherical diameter in a range of 3.27 μm to 7.96 μm were identified as *E. huxleyi*, after microscopic inspection. Steady state was assumed when variations in cell abundance were <10% for 3 consecutive days (Leonardos & Geider 2005).

Chlorophyll a. Concentrations of chlorophyll a (chl a) were determined by ion-pairing reverse-phase high-pressure liquid chromatography (HPLC) after extraction into acetone (Mantoura & Llewellyn 1983, Bidigare et al. 1985, Sun et al. 1991). Briefly, duplicate 20 ml samples from each chemostat were filtered onto combusted GF/F filters; samples were frozen until analysis. To extract chl a, the filters were sonicated in HPLC-grade acetone; 2 successive 5 ml extracts were combined and filtered through a 0.2 μm Zetapor membrane. Samples were covered with aluminum foil to protect them from light during handling and analysis. Chl a was separated from other chloropigments by HPLC on a 5 μm Adsorbosphere C-18 column as described by Sun et al. (1991). Chl a was detected by fluorescence (excitation $\lambda = 440$ nm, emission $\lambda = 660$ nm), and was quantified using an authentic standard (Turner).

Bacterial cell counts. Samples (4.5 ml) were preserved with glutaraldehyde (GDA, AppliChem, 1.1% v/v final concentration), and stored at -20°C for 3 mo until flow cytometry analysis using a FACS Calibur flow cytometer (Becton Dickinson) following the method of Gasol & Del Giorgio (2000). Briefly, nucleic acids in the bacteria were stained with SybrGreen I (Invitrogen). The stock solution of SybrGreen I (10000 \times) was diluted 1:40 with dimethyl sulfoxide (DMSO, Sigma Aldrich), followed by a 1:40 dilution with the sample (final dilution 10^{-3} , final concentration 6.25 \times). Shortly before analysis, thawed samples were incubated for 30 min in the dark. As an internal standard, yellow-green fluorescent latex beads (0.94 μm diameter, Polyscience) were used for the volume normalization of counted events. Bacterial cell numbers were calculated using Cell Quest Pro software.

POC, PIC, PN, and POP. Particulate C and N contents were run in duplicate using a Carlo Erba EA-1112 CNS analyzer. For this analyzer, the level of uncertainty is $\pm 2\%$ for C and $\pm 5\%$ for N analysis. Inorganic carbon was removed using 10% HCl, and

PIC was calculated as the difference between TPC (total particulate carbon) and POC. For POP, 30 to 80 ml of sample was filtered gently (<200 mm Hg) onto combusted GF/F filters. POP was determined colorimetrically after persulfate oxidation of POP with a precision of $\pm 0.02 \mu\text{mol l}^{-1}$ (Koroleff & Grasshof 1983).

Nutrients. Samples were filtered through 0.2 μm syringe filters and frozen at -20°C until analysis. Measurements of NO_3^- , NO_2^- , NH_4^+ and PO_4^{3-} were made spectrophotometrically after Grasshof et al. (1999) using an Evolution 3 autoanalyzer (Alliance Instruments). Detection limits were 0.3 $\mu\text{mol l}^{-1}$ for N and 0.01 $\mu\text{mol l}^{-1}$ for P.

Transparent exopolymer particles (TEP). TEP were detected by staining with Alcian Blue, a cationic copper phthalocyanine dye that complexes carboxyl ($-\text{COO}^-$) and half-ester sulfate (OSO_3^-) reactive groups of acidic polysaccharides. The amount of Alcian Blue adsorption per sample volume is a measure of TEP concentration, and was determined colorimetrically according to Passow & Alldredge (1995) from 50 to 100 ml samples filtered onto 0.4 μm Nuclepore filters. All filters were prepared in duplicate. Microscopic analysis of TEP size and abundance was performed after Engel (2009). Semi-permanent slides (CytoClear) were prepared by filtration (<200 mbar) of 5 to 10 ml samples onto 0.4 μm Nuclepore filters (25 mm) and the TEP stained with 1 ml Alcian Blue. All filters were prepared in duplicate and stored frozen at -20°C until analysis. TEP slides were examined using a compound light microscope and a digital AxioCam HRc camera (Zeiss) with 200 to 400 \times magnification. Microscopic inspection revealed only stained coccospheres and no 'free' TEP present, so further microscopic analysis of TEP slides was discontinued.

Dissolved organic carbon (DOC). Samples for DOC (20 ml) were collected in combusted glass ampoules after filtration through combusted GF/F filters. Samples were acidified with 100 μl of 85% phosphoric acid, heat sealed immediately, and stored at 4°C in the dark until analysis. DOC samples were analyzed using the high-temperature combustion method (TOC-VCSH, Shimadzu) (Qian & Mopper 1996). A multi-point calibration curve was prepared each day of measurement using a potassium hydrogen phthalate standard prepared in MilliQ water. Additionally, 2 reference seawater standards (from Dennis Hansell, RSMAS, University of Miami) were used to determine the instrument blank. Each sample was measured in quadruplicate.

Total dissolved nitrogen (TDN). TDN was determined simultaneously with DOC using the TNM-1

detector on the Shimadzu analyzer. TDN is combusted and converted to NO_x, which chemiluminesces when mixed with ozone and can be detected using a photomultiplier (Dickson et al. 2007). DON was calculated from TDN by subtraction of NO₃⁻, NO₂⁻, and NH₄⁺ concentrations.

Data analysis. Differences in data as revealed by statistical tests (*t*-test, ANOVA Kruskal-Wallis One Way Analysis of Variance on Ranks, Kolmogorov-Smirnov test) were accepted as significant for $p < 0.05$. Average values for total concentrations are given by their arithmetic mean ± 1 standard deviation (SD), averages for ratios by their geometric mean. Calculations, statistical tests and illustration of the data were performed with the software packages Microsoft Office Excel 2010 and Sigma Plot 12.0 (Systat).

RESULTS

Chemostat nutrient and carbonate chemistry

Nitrate and phosphate were below detection levels in all samples. Nitrite concentration was 0.15 to 0.16 $\mu\text{mol l}^{-1}$ and did not differ significantly between CO₂ treatments.

Throughout the steady-state period, average pH was 8.46 ± 0.08 (180 μatm), 8.24 ± 0.06 (380 μatm) and 8.02 ± 0.07 (750 μatm) (Fig. 2a). TA was not significantly different between treatments, yielding 2400 ± 206 (180 μatm), 2473 ± 226 (280 μatm), and 2450 ± 255 (760 μatm) $\mu\text{mol l}^{-1}$. Calculations of $p\text{CO}_2(\text{aq})$ from pH and TA yielded values of 190 ± 53 (180), 377 ± 28 (380), and 647 ± 69 (750) μatm (Fig. 2b). Both $p\text{CO}_2(\text{aq})$ and pH differed significantly between the treatments during the steady-state period as well as during the entire experiment (ANOVA, $p < 0.01$). Calcite saturation ($\Omega\text{-Ca}$) was 6.36 ± 0.42 (180 μatm), 4.27 ± 0.49 (380 μatm), and 2.83 ± 0.57 (750 μatm) on average and hence > 2 in all samples (Fig. 2c).

Cell abundance and state-steady growth

Emiliana huxleyi was grown inside the chemostat chambers in batch mode for 5 d. Flow through the chemostat was started on Day 6 and run for ca. 3 wk at a rate of $D = 0.2 \text{ d}^{-1}$ until steady state was achieved on Day 28; sampling began on Day 30 (Fig. 1). As expected, cell concentrations initially decreased when chemostat flow began, but after 1 week increased again towards steady state. After Day 28, temporal

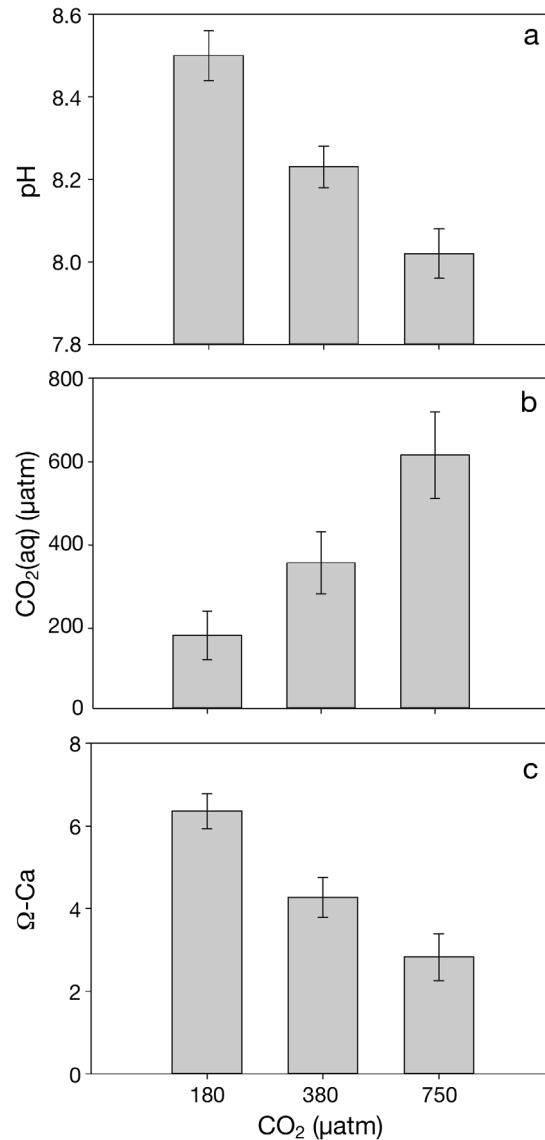


Fig. 2. Variations of (a) pH, (b) CO₂(aq), and (c) calcite saturation state ($\Omega\text{-Ca}$) strongly differed during the steady state phase of the *Emiliana huxleyi* chemostat experiment adjusted to 180, 380 and 750 μatm CO₂. Error bars: ± 1 SD, $n = 5$ for 180 μatm and $n = 10$ for 380 and 750 μatm

variation of cell abundance within each chemostat was $< 10\%$, defining steady-state cell growth. Cell abundance at the 3 CO₂ concentrations was not significantly different between treatments: $4.8 \pm 0.85 \times 10^8 \text{ l}^{-1}$ (180 μatm), $4.8 \pm 1.0 \times 10^8 \text{ l}^{-1}$ (380 μatm) and $5.3 \times 10^8 \text{ l}^{-1} \pm 9.16 \times 10^7$ (750 μatm) (Fig. 3a). No significant difference between treatments was observed in the chl *a* content of *E. huxleyi* cells (Fig. 3b). Numbers of heterotrophic bacteria varied between $2 \times 10^9 \text{ l}^{-1}$ and $3 \times 10^9 \text{ l}^{-1}$, also with no CO₂ effect. The number of bacteria during this experiment was rela-

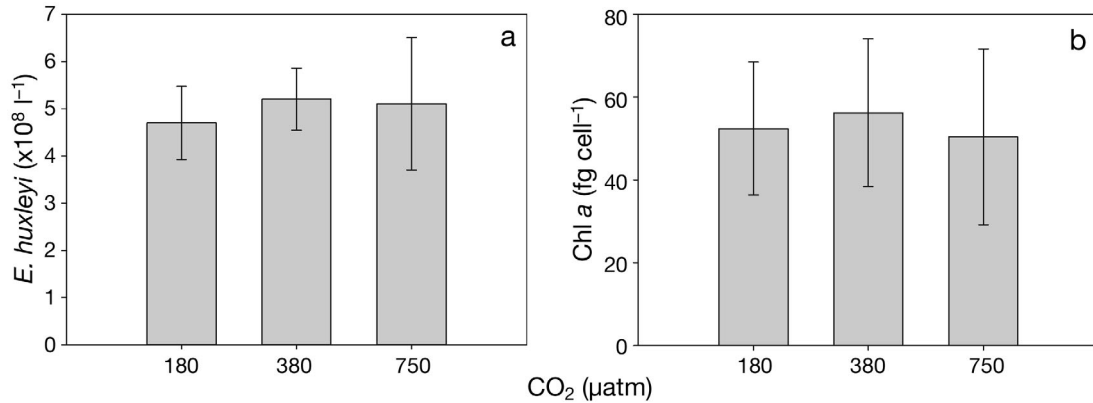


Fig. 3. No significant differences were observed in (a) the abundance of *Emiliana huxleyi* cells or (b) the chlorophyll a (chl a) content of cells during the steady-state phase of the chemostat experiments adjusted to 180, 380 and 750 µatm CO₂. Error bars: ± 1 SD, n = 5 for 180 µatm and n = 10 for 380 and 750 µatm

tively high and can be attributed to the long duration of the experiment and to the large volume of water required for continuous culture. However, estimating a bacterial cell quota of 30 fg C, 5 fg N and 1.4 fg P (upper level for natural marine bacteria given in Fagerbakke et al. 1996), bacteria contributed at most 1 to 2% POC, 3 to 4% PN and 7 to 10% POP. Because the impact of bacteria on element stoichiometry during this study was therefore presumably small, and element quotas of bacteria are highly variable, both within and between species, bacterial contribution to POC, PN and POP will not be resolved in this study.

Biogeochemical composition

Concentrations of particulate elements are shown in Table 1. Particulate C, N and P in chemostats at the 3 levels of CO₂ were normalized to cell abundance and compared for the steady state period of observation. Average cell quotas ranged from 1.3 to 1.5 pmol PIC cell⁻¹ (Fig. 4a), 0.79 to 0.82 pmol POC cell⁻¹ (Fig. 4b), 0.048 to 0.053 pmol PN cell⁻¹ (Fig. 4c) and 2.8 to 3.2 fmol POP cell⁻¹ (Fig. 4d). No significant differences between CO₂ treatments were observed for any of the cell quotas. The spread in elemental concentrations and cell quotas for each CO₂ treatment represents the variability over time during the steady state growth period sampled. Variability of cell quotas within each treatment differed between elements. Lowest within-treatment variability was observed for the cell quota of POC, followed by PIC, PN and POP.

Table 1. Average concentrations and specific variations in particulate organic matter (POM)—inorganic carbon (PIC), organic carbon (POC), nitrogen (PON) and phosphorus (POP)—at different levels of CO₂, determined at 5 different time-points over a period of 14 d in phosphorus-limited chemostats. Duplicate chemostats were used for 380 and 750 µatm treatments

POM (µmol l ⁻¹)	180 µatm (avg.; n = 5) SD (%)		380 µatm (avg.; n = 10) SD (%)		750 µatm (avg.; n = 10) SD (%)	
POC	399	14	401	17	418	19
PIC	645	18	715	33	700	16
PON	24.2	11	24.4	8	24.6	9
POP	1.59	40	1.36	37	1.49	32

Concentrations of DOC and DON in the initial culture medium averaged $183 \pm 0.1 \mu\text{mol C l}^{-1}$ and $20 \pm 4.8 \mu\text{mol N l}^{-1}$, respectively. Concentrations were higher inside the chemostat by about $7 \mu\text{mol DOC l}^{-1}$ and $2 \mu\text{mol DON l}^{-1}$, indicating net biological production. No significant influence of the CO₂ treatment was observed on concentrations of DOC (Fig. 5a) or DON (Fig. 5b). Instead, both components of dissolved organic matter were remarkably stable over time and very similar in all chemostats. For dissolved organic components, variability over time was generally lower than for particulate components (Table 1), i.e. 2.9 to 7.5% for DOC and 2.6 to 3.3% for DON.

Concentration ratios determined during the study are depicted in Fig. 6a-d. As was the case for individual components, no significant influence of CO₂ treatment was determined for any of the following ratios: [PIC]:[POC], [POC]:[PN], [PN]:[POP] or [DOC]:[DON]. Average ratios of [PIC]:[POC] ranged between 1.6 and 1.8, indicating fully calcified cells in all treatments. Average ratios of [POC]:[PN] varied between 16.6 and 17.2, and were clearly above the Redfield ratio of 6.6 throughout the study. Average

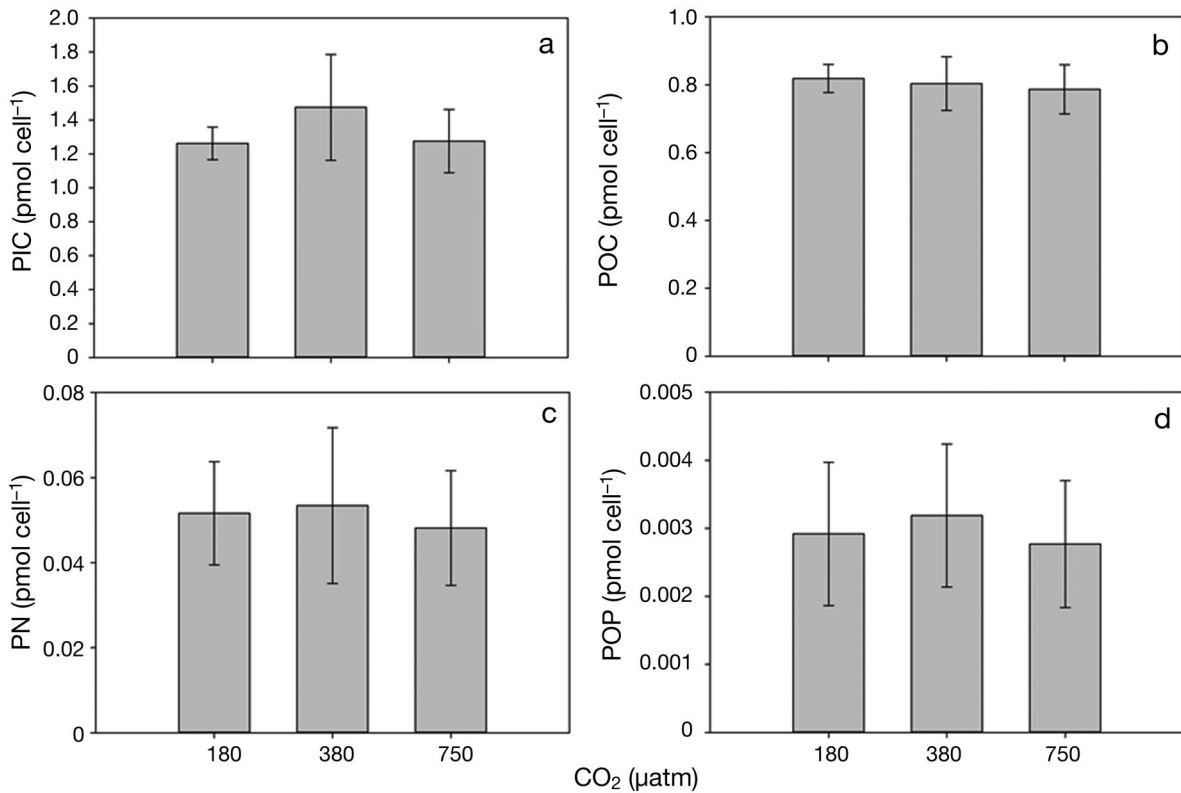


Fig. 4. Variations of particulate (a) inorganic carbon (PIC), (b) organic carbon (POC), (c) nitrogen (PN) and (d) organic phosphorus (POP) were normalized to *Emiliana huxleyi* cell abundances and did not differ significantly in chemostats adjusted to 180, 380 and 750 μatm CO₂. Error bars: ±1 SD, n = 5 for 180 μatm and n = 10 for 380 and 750 μatm

[PN]:[POP] ratios were 17.3 to 19.7 and higher than the Redfield ratio of 16 (*t*-test, *p* = 0.06 for samplings Days 30 to 44; *p* < 0.001 for samplings Days 34 to 44), reflecting the relative P shortage applied in the nutrient media (Fig. 6c). Ratios for [DOC]:[DON] ranged between 8.4 and 8.6 (Fig. 6d) and were thus clearly lower than [POC]:[PN] ratios, albeit still above the Redfield reference value.

TEP

No individual gel particles were observed by microscopic examination throughout the steady-state phase in any of the chemostats. It has been shown that coccoliths of *E. huxleyi* include an acidic polysaccharide that adsorbs Alcian Blue (de Jong et al. 1976, Fichtinger-Schepman et al. 1979). This poly-

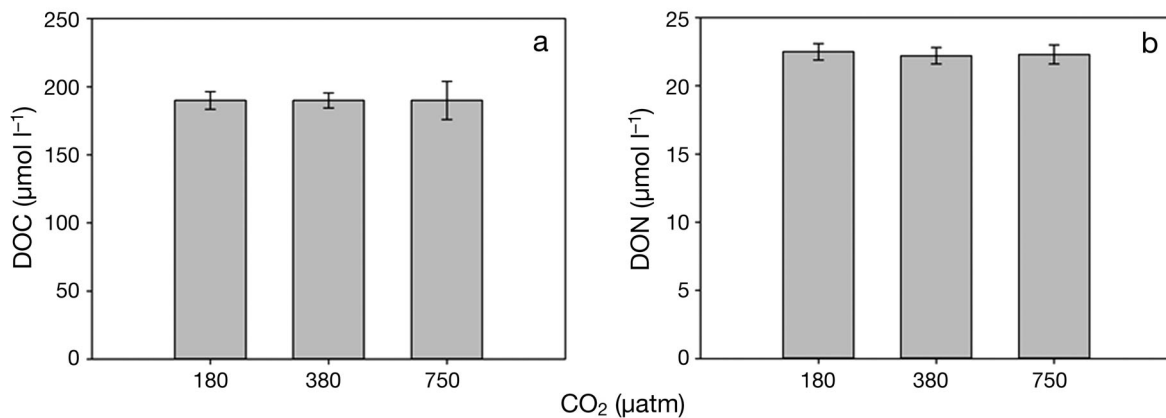


Fig. 5. Concentrations of (a) dissolved organic carbon (DOC) and (b) dissolved organic nitrogen (DON) during the steady-state phase of the *Emiliana huxleyi* chemostat experiment were very similar between CO₂ treatments. Error bars: ±1 SD, n = 5 for 180 μatm and n = 10 for 380 and 750 μatm.

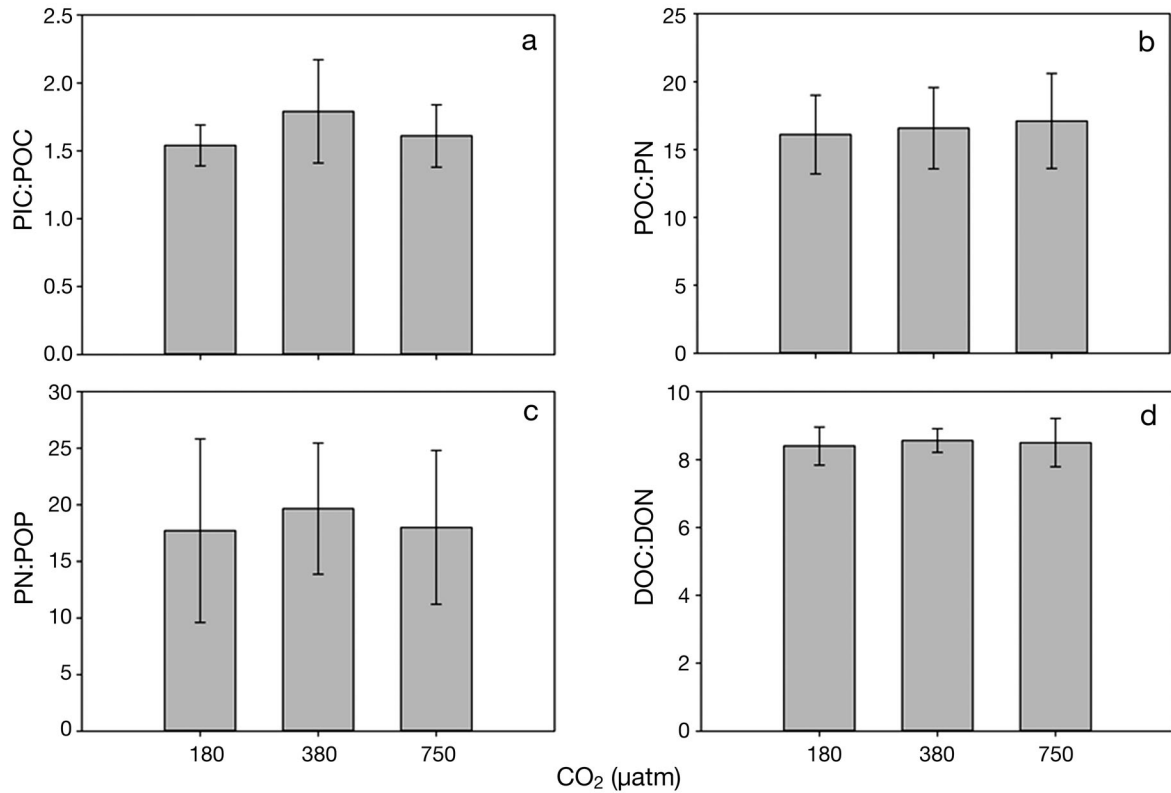


Fig. 6. Element ratios determined during steady state growth of *Emiliana huxleyi* did not differ significantly between CO₂ treatments for (a) PIC:POC, (b) POC:PN, (c) PN:POP, or (d) DOC:DON. Error bars: ± 1 SD, $n = 5$ for 180 μatm and $n = 10$ for 380 and 750 μatm

saccharide is assumed to play a role in the biomineralisation process and probably also in the agglutination of coccoliths in the coccosphere (Van Emburg et al. 1986). Engel et al. (2004b) showed that the amount of Alcian Blue dye adsorption (AB_{ad}) in exponentially growing, nutrient-replete *E. huxleyi* cultures without TEP was directly related to cell abundance, equivalent to 2.55 ± 0.4 pg Xanthan equivalents ($\text{X}_{\text{eq. cell}^{-1}}$). During this study, a significant linear relationship between AB_{ad} and cell abundance was also observed ($p < 0.01$; data not shown), yielding $\Delta[\text{AB}_{\text{ad}}]: \Delta[\text{cell}]$ of 3.6 ± 0.02 pg $\text{X}_{\text{eq. cell}^{-1}}$. This slightly higher value may be attributable to the high degree of calcification determined during this study, but is still low compared to previous mesocosms or culture studies that showed production of TEP by *E. huxleyi* (Engel et al. 2004b, Harlay et al. 2009, Borchard & Engel 2012), and in accordance with the observed absence of TEP during this study.

DISCUSSION

During this study, the growth rate of *Emiliana huxleyi* was controlled by the flow rate in our chemo-

stats, which was maintained at steady state (0.2 d^{-1}). The relatively long period (30 d) that cells grew in the chemostat under constant conditions before sampling allowed cells to acclimate to their environment, specifically to the low supply of phosphate. Element cell quotas and stoichiometry under these growing conditions were insensitive to different $p\text{CO}_2$ levels, indicating that PIC, POC, PN and POP were primarily constrained by the nutrient and light regime (equal in all treatments). It has been suggested that environmental co-factors such as light and nutrient availability may alter the response of *E. huxleyi* to CO₂ changes. We will therefore discuss whether these cofactors may have attenuated cell response to CO₂ during this study.

Light as a cofactor

The amount of energy, i.e. light, available for metabolic processes may play a role in whether *E. huxleyi* is sensitive to changes in $p\text{CO}_2$ (Zondervan 2007, Raven & Crawford 2012). Zondervan et al. (2002) observed no response of calcification to CO₂ when cells were grown at low light ($< 100 \mu\text{E m}^{-2} \text{ s}^{-1}$). Rokitta &

Rost (2012a) also observed a stronger decrease in PIC per cell for *E. huxleyi* at high compared to low light. During our study, light was not limiting, as the available $190 \mu\text{E m}^{-2} \text{s}^{-1}$ is close to the light saturation level of $200 \mu\text{E m}^{-2} \text{s}^{-1}$ reported for *E. huxleyi* by Nielsen (1997). Zondervan et al. (2002) observed highest, i.e. light-saturated, growth rates at $150 \mu\text{E m}^{-2} \text{s}^{-1}$ at 15°C —a temperature similar to that used during this study (14°C). This suggests that irradiance applied during this study was not limiting cell growth, and not low enough to account for the observed absence of a CO_2 effect on element stoichiometry.

Nutrients as cofactors

Another factor potentially modulating CO_2 responses is nutrient availability. During our chemostat study, the culture medium was nutrient-depleted. Phosphate limitation has been shown to increase the number of coccolith platelets per cell, resulting in higher [PIC]:[POC] (Paasche 1998, Riegman et al. 2000). Cell quotas determined during this study were $>1 \text{ pmol PIC cell}^{-1}$ and thus relatively high compared to cells growing in nutrient-replete conditions, i.e. 0.25 to $0.87 \text{ pmol PIC cell}^{-1}$ (e.g. Riebesell et al. 2000a, Lohbeck et al. 2012, Iglesias-Rodriguez et al. 2008a), or in nitrogen-limited cultures ($\sim 0.16 \text{ pmol IC cell}^{-1}$) (Müller et al. 2012). Moreover, [PIC]:[POC] was always above 1, reflecting a high degree of calcification. These findings are in accordance with earlier findings showing that [PIC]:[POC] can rise from below 1 up to 2.2 under phosphate limitation (Paasche 2001). Using a similar experimental set-up, Borchard et al. (2011) also observed no effect of CO_2 aeration on C and N quotas of *E. huxleyi* under phosphate-limited growth at 0.3 and 0.1 d^{-1} . An attenuated effect of $p\text{CO}_2$ on element ratios of *E. huxleyi* was observed for cells grown under high [N]:[P] by Matthiessen et al. (2012). Thus, phosphorus limitation may be a factor in the suppression of CO_2 effects on element stoichiometry. This may be highly relevant for estimating future changes in the ocean's biogeochemical cycling due to CO_2 responses of *E. huxleyi*, as this species is known to become abundant and form blooms in low-nutrient waters, especially when [N]:[P] is high (Tyrrell & Merico 2004).

In chemostat studies where cultures were limited by nitrogen rather than phosphorus, a different pattern is seen. Sciandra et al. (2003a) grew *E. huxleyi* in continuous culture at light intensities ($170 \mu\text{E m}^{-2} \text{s}^{-1}$) similar to our experiments, but under N-limitation

and at a higher growth rate (0.5 d^{-1}). They observed an immediate response of cells to changes in $p\text{CO}_2$ and a decrease in net calcification and photosynthesis rates, yielding, however, no effect of $p\text{CO}_2$ on [PIC]:[POC]. Also during N-limited growth in chemostats, Müller et al. (2012) observed a decreasing trend in [PIC]:[POC], and an increasing trend in [POC]:[POP] and [TPN]:[POP] with $p\text{CO}_2$, whereas [POC]:[PN] was unaffected by CO_2 . Thus, nitrogen limitation may not suppress CO_2 sensitivities of *E. huxleyi*.

Transient versus steady state growth

Rokitta & Rost (2012a) emphasized that in previous studies of *E. huxleyi* grown at present CO_2 levels (or higher), the TPC content remained stable despite a change in PIC and POC quotas. A decrease in PIC was associated with an increase in POC or vice versa. They concluded that stable TPC production, in spite of different $p\text{CO}_2$ levels, suggests that overall CO_2 uptake does not change, but that the carbon is allocated between POC and PIC differently under ocean acidification. In our study, PIC and POC cell quotas were rather constant over time and similar between $p\text{CO}_2$ treatments. This suggests that *E. huxleyi* is in principle capable of acclimating to different CO_2 concentrations, so that no differences in its cellular elemental content could be resolved during this experiment. Steady state (balanced) growth, i.e. growth at a defined rate, over an extended period is a prerequisite to investigate the physiological response of cells to a limiting factor. On the one hand, the chemostat system is therefore more advantageous than the batch approach, where growth rates and environmental conditions, like nutrient supply, are constantly changing (Jannasch 1974, Langer et al. 2013). On the other hand, balanced growth conditions are hardly met in a natural environment. In nature, cell growth is a transient process and the cell's physiology is dynamic, constantly pursuing optimum conditions for growth. A CO_2 effect may therefore be related to the cell's physiological ability to respond to a changing microenvironment.

One important process in this respect is the partitioning of metabolic products under nutrient-limiting conditions. For *E. huxleyi*, it has been shown that an increase in POC production under nutrient limiting conditions was associated with the production of extracellular particulate organic carbon, such as TEP (de Bodt et al. 2008, Borchard & Engel 2012). An increase in TEP concentration was also part of the

explanation for increasing POC concentrations during mesocosm studies with and without $p\text{CO}_2$ alterations (Engel et al. 2002, Engel et al. 2004b). Other studies have revealed that TEP formation increases with increasing ocean acidification (Engel 2002, Mari 2008, Borchard & Engel 2012). It is known that CO₂ can alleviate rate limitation of primary production in phytoplankton, such as *E. huxleyi*, that are inefficient in carbon acquisition (Rost et al. 2003). Higher $p\text{CO}_2$ in exponentially growing cells can therefore support higher primary production that, under nutrient limitation, is exuded in the form of carbohydrates, eventually forming TEP.

Production of TEP is viewed as a carbon 'overflow' for photosynthesis products under nutrient depletion. Schartau et al. (2007) showed that in a model study the production of organic carbon in excess of nitrogen uptake and Redfield stoichiometry, frequently referred to as 'carbon overconsumption' (Toggweiler 1993), can be split into 2 types. The first type explains a small amount of excess carbon uptake during exponential growth. This excess carbon is well allocated within the cell and contributes to changes in cell quota while the release of carbohydrates remains small. The second type is a transient phenomenon that occurs when nutrients limit cell growth. In this case, the carbon assimilation is too extreme and cannot be allocated within the cell to promote growth. The cells are in a state of severe acclimation, and excessive carbon is released as carbohydrates. This transient period of growth limitation is largely determined by the timescale of possible physiological acclimation. Obviously, it is this transient growth phase where we must expect the largest sensitivity in TEP formation to variations in $p\text{CO}_2$. Our chemostat experiment does not cover a transient growth period, which could explain the observed negligible TEP concentrations.

Comparison with previous studies

The absence of a clear CO₂ signal on element composition or TEP production during our study does not necessarily imply the absence of a CO₂ effect on *E. huxleyi* in general, but demands a more careful consideration of (short-term) variations in growth history. For example, comparable low growth rates can be achieved under steady state conditions, or they can occur during the course of a bloom experiment, e.g. when approaching nutrient depletion. Both situations differ with respect to the cell's physiological acclimation state and likely

exhibit different sensitivities to environmental variations such as in $p\text{CO}_2$.

Previous studies of CO₂ effects on growth and calcification of *E. huxleyi* differed in their experimental design and covered diverse growing conditions, including transient growth phases. Since we would not expect transient growth periods to happen during experiments with sufficient nutrient supply and high growth rate, we anticipated larger differences in elemental content between independent studies at lower rather than at high growth rates. Likewise, studies that included periods of physiological acclimation, i.e. due to nutrient limitation, should have shown larger differences in elemental content between different $p\text{CO}_2$ conditions than those studies where high growth rates were maintained by nutrient saturation.

To compare our results of growth under steady-state conditions with previous findings, we compiled published data of PIC and POC divided by the corresponding cell abundance of *E. huxleyi* at various $p\text{CO}_2$ levels and growth rates. The collected data originate from 20 independent studies, of which 17 datasets were retrieved from the EPOCA database; www.epoca-project.eu/index.php/data/data-sets.html (Fig. 7a-d). The pH levels in these studies cover a wide range, from 7.09 ($p\text{CO}_2 \approx 5869 \mu\text{atm}$) to 9.12 ($p\text{CO}_2 \approx 28 \mu\text{atm}$). Observed growth rates varied between 0.01 and 1.67 d⁻¹ (Fig. 7a). The dataset was split into an upper and lower range of relative growth rates (RGR). The separation is defined at RGR = 0.8 d⁻¹, which approximates the middle of the variational growth range and splits data into 2 subsets of comparable size ($n = 178$ for RGR > 0.8 d⁻¹ and $n = 220$ for RGR < 0.8 d⁻¹). In addition, we differently labeled data subsets according to their pH variational range. Mean pH of all measurements was $\overline{\text{pH}} = 8.04$, with a standard deviation of $\sigma = 0.25$. The upper range considered data with $\text{pH} > 8.29 = \overline{\text{pH}} + \sigma$, the middle range included data that fulfilled $\text{pH} < \overline{\text{pH}} \pm \sigma < \text{pH}$, and data with pH below 7.79 ($\overline{\text{pH}} - \sigma < 7.79$) (Fig. 7a). The purpose of splitting data into smaller subsets was to visually accentuate how variability in POC and PIC cell quotas and the corresponding [PIC]:[POC] depended on RGR and pH (Fig. 7b-d).

The compiled PIC and POC cell quotas with RGR > 0.8 d⁻¹ were normally distributed with median \approx mean = $0.9 \pm 0.2 \text{ pmol cell}^{-1}$ for POC and median \approx mean = $0.7 \pm 0.2 \text{ pmol cell}^{-1}$ for PIC. Likewise, the corresponding distribution of [PIC]:[POC] values was normal (median \approx mean = $0.8 \pm 0.2 \text{ pmol cell}^{-1}$). Cell quotas of POC and PIC with RGR < 0.8 d⁻¹ revealed much greater variability, emphasizing

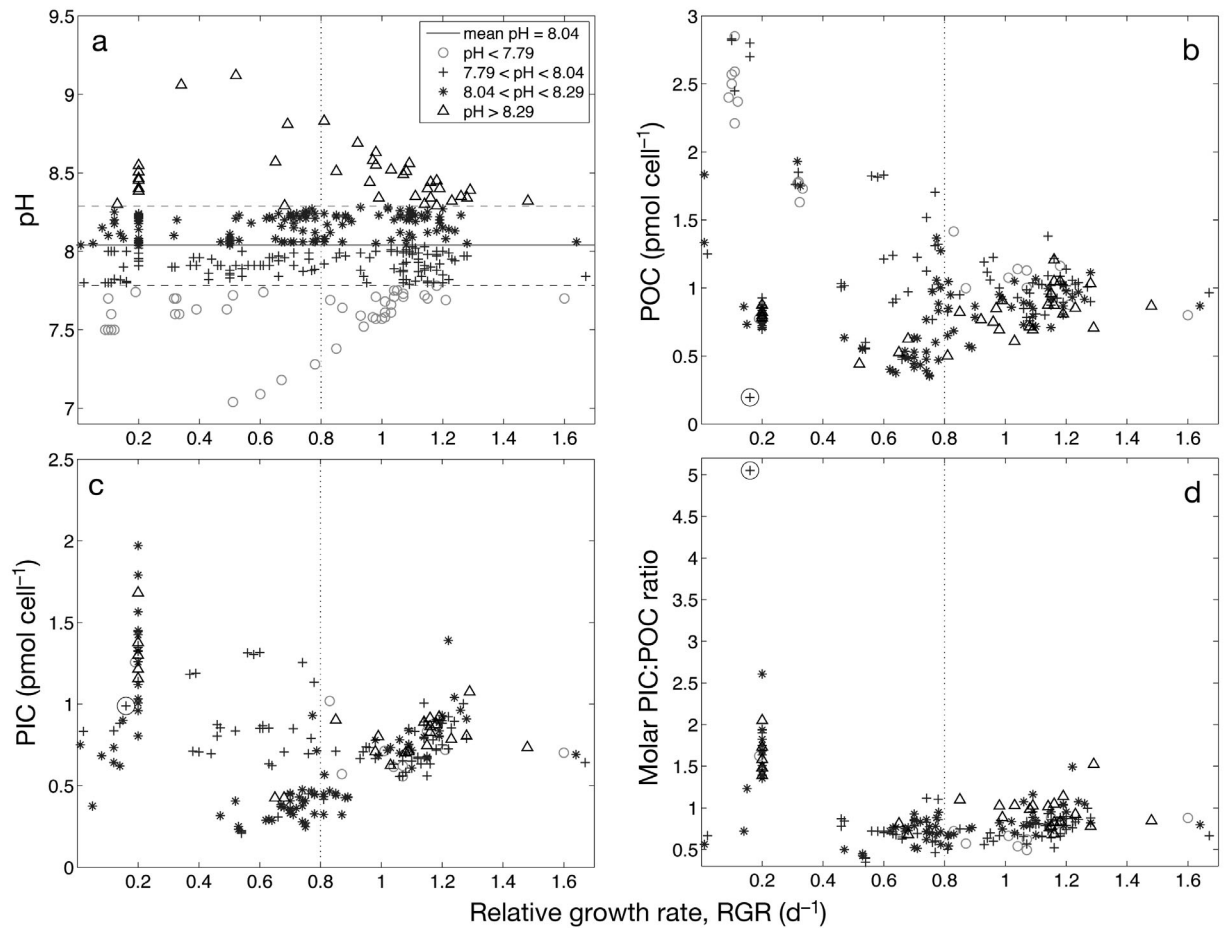


Fig. 7. Compiled dataset for *Emiliana huxleyi* split according to the 4 pH ranges applied during these studies; plotted against relative growth rate (RGR) are (a) pH, (b) POC normalized to cell abundance, (c) PIC normalized to cell abundance, and (d) [PIC]:[POC] molar ratios. Solid and dashed lines indicate mean pH and mean pH \pm standard deviation ($\mu \pm \sigma$ pH), respectively. Vertical dotted lines mark the separation of data into subsets of $RGR < 0.8 \text{ d}^{-1} < RGR$, explanation in text. Data included from: Biermann & Engel (2012), Borchard et al. (2012), Barcelos e Ramos et al. (2010), Richier et al. (2011), Koch (2010), Iglesias-Rodríguez et al. (2008b), Langer et al. (2009b), Lefebvre et al. (2011), Riebesell et al. (2000a,b), Sciandra et al. (2003b), Fiorini et al. (2010), Bach et al. (2011), de Bodt et al. (2010b), Fiorini et al. (2011), Hoppe et al. (2011), Müller et al. (2010), Rokitta & Rost (2012b), Lohbeck et al. (2012), and the present study. One data point was encircled as an outlier due to its very low C-quota

physiological variations with different impacts on element stoichiometry. At low RGR ($< 0.8 \text{ d}^{-1}$), the subset of POC and PIC measurements deviated from their means, with more data exhibiting elevated values. For example, the data subset that corresponded with the lower pH range ($\text{pH} < 7.79$) included up to threefold higher values than the mean value observed at $RGR > 0.8 \text{ d}^{-1}$. For $RGR < 0.4 \text{ d}^{-1}$ and $\text{pH} < 7.79$ in particular, POC quotas were significantly higher at high $p\text{CO}_2$ levels, with values between 1.6 and 2.9 pmol cell^{-1} , which is well above the median value of 0.92 pmol cell^{-1} (Fig. 7b). Under low $p\text{CO}_2$ conditions ($\text{pH} > 8.26$), we found no POC above 1.2 pmol cell^{-1} , and all values for $RGR < 0.8 \text{ d}^{-1}$ were below the respective reference median of $RGR > 0.8 \text{ d}^{-1}$. The medium pH

ranges ($7.79 < \text{pH} < 8.04$ and $8.04 < \text{pH} < 8.29$) included POC measurements that ranged from 0.2 up to 1.9 pmol cell^{-1} . PIC data showed similar behavior compared to POC, but with one exception: elevated PIC values between 1.1 and 1.7 pmol cell^{-1} , i.e. higher than the reference average of 0.7 pmol cell^{-1} , were also observed under low $p\text{CO}_2$ conditions ($\text{pH} > 8.26$) at low RGR. These values yielded elevated [PIC]:[POC] between 1.4 and 2.0 (Fig. 7d), and encompassed the range observed during this study. For *E. huxleyi*, elevated [PIC]:[POC] at low RGR can be explained by (1) an increasing number of calcite platelets per cell when cell growth ceases while calcification continues, and (2) a harvest of detached coccoliths after they have been shed by growth-limited cells of growth-limited cultures dur-

ing sampling. At higher RGR, cell quotas of PIC and POC revealed similar trends, yielding no clear difference of [PIC]:[POC] between pH settings.

Overall, the variability seen in these subsets makes the extraction of a generic CO₂ response signal difficult, if not impossible. To approach this, further details about differences between experimental setups are required to untangle variations in growth condition. Experimental settings of the compiled dataset shown in Fig. 7 include variations in *p*CO₂, temperature, light, species strain, nutrient stoichiometry, and growth rate as well as data from chemostats and batch cultures. To deduce a clear response signal in PIC or POC quotas due to *p*CO₂ or pH change remains difficult, particularly for the medium pH range (7.79 < pH < 8.29) that may be representative of future ocean acidification (Frölicher & Joos 2010). Here, element quotas are seemingly highly sensitive to a variety of environmental conditions and vary with RGR. Data obtained during our chemostat study fall well within the range of the previous observations, but no direct effect of *p*CO₂ on elemental stoichiometry of *E. huxleyi* was observed while RGR was constant. With respect to climate change, variations in the spatial and temporal distribution of *E. huxleyi* will occur in association with changes in temperature, nutrient availability, grazing pressure, and ocean acidification. A better understanding of the cell's physiological constraints to optimize resources, i.e. element uptake and incorporation, and to acclimate to a heterogeneous and continuously changing environment, might be necessary before we can truly estimate the future response of elemental composition of *E. huxleyi* to environmental stressors such as ocean acidification.

Acknowledgements. This research was supported by the Helmholtz foundation (HZ-NG-102), the Federal Ministry of Education and Research (BMBF, FKZ 03F0608) through the BIOACID (Biological Impacts of Ocean ACIDification) project, and the Chemical Oceanography Program of the US National Science Foundation through the ADAGIO Project. We thank Nicole Händel, Karin Woudsma and Laura Wischnewski for nutrient analyses, Corinna Borchard for POP measurements, and Jon Roa and Nicole Händel for DOC and TDN analyses.

LITERATURE CITED

- Aksnes DL, Egge JK (1991) A theoretical model for nutrient uptake in phytoplankton. *Mar Ecol Prog Ser* 70:65–72
- Aksnes DL, Egge JK, Rosland R, Heimdal BR (1994) Representation of *Emiliana huxleyi* in phytoplankton simulation models. A first approach. *Sarsia* 79:291–300
- Bach LT, Riebesell U, Schulz KG (2011) Seawater carbonate chemistry, growth rate and PIC and POC production during experiments with *Emiliana huxleyi* (B92/11), doi: 10.1594/PANGAEA.771288
- Barcelos e Ramos J, Müller M, Riebesell U (2010) Seawater carbonate chemistry and processes during experiments with phytoplankton *Emiliana huxleyi* (strain Bergen 2005), doi:10.1594/PANGAEA.736022
- Beardall J, Raven JA (2004) The potential effects of global climate change on microalgal photosynthesis, growth and ecology. *Phycologia* 43:26–40
- Biddanda B, Benner R (1997) Carbon, nitrogen, and carbohydrate fluxes during the production of particulate dissolved organic matter by marine phytoplankton. *Limnol Oceanogr* 42:506–518
- Bidigare RR, Kennicutt MC, Brooks JM (1985) Rapid determination of chlorophylls and their degradation products by high-performance liquid chromatography. *Limnol Oceanogr* 30:432–435
- Biermann A, Engel A (2012) Seawater carbonate chemistry and its effects on properties and sinking velocity of aggregates of the coccolithophore *Emiliana huxleyi*, doi:10.1594/PANGAEA.778432
- Borchard C, Engel A (2012) Organic matter exudation by *Emiliana huxleyi* under simulated future ocean conditions. *Biogeosciences* 9:3405–3423
- Borchard C, Borges AV, Händel N, Engel A (2011) Biogeochemical response of *Emiliana huxleyi* (PML B92/11) to elevated CO₂ and temperature under phosphorous limitation: a chemostat study. *J Exp Mar Biol Ecol* 410:61–71
- Borchard C, Borges AV, Händel N, Engel A (2012) Seawater carbonate chemistry and biological processes of *Emiliana huxleyi* (PML B92/11) during experiments, doi: 10.1594/PANGAEA.774802
- Brewer PG, Goyet C, Friedrich G (1997) Direct observation of the oceanic CO₂ increase revisited. *Proc Natl Acad Sci USA* 94:8308–8313
- Chen GT, Millero FJ (1979) Gradual increase of oceanic CO₂. *Nature* 277:205–206
- de Bodt C, Harlay J, Chou L (2008) Biocalcification by *Emiliana huxleyi* in batch culture experiments. *Mineralogical Magazine* 72:251–256
- De Bodt C, Van Oostende N, Harlay J, Sabbe K, Chou L (2010a) Individual and interacting effects of *p*CO₂ and temperature on *Emiliana huxleyi* calcification: study of the calcite production, the coccolith morphology and the coccosphere size. *Biogeosciences* 7:1401–1412
- de Bodt C, Van Oostende N, Harlay J, Sabbe K, Chou L (2010b) Seawater carbonate chemistry, growth rate and *Emiliana huxleyi* (strain AC481) biological processes during experiments, doi:10.1594/PANGAEA.772696
- de Jong EW, Bosch L, Westbroek P (1976) Isolation and characterization of a Ca²⁺-binding polysaccharide associated with coccoliths of *Emiliana huxleyi* (Lohmann) Kamptner. *Eur J Biochem* 70:611–621
- Dickson AG, Millero FJ (1987) A comparison of the equilibrium constants for the dissociation of carbonic acid in seawater media. *Deep-Sea Res Part I* 34:1733–1743
- Dickson AG, Wesolowski DJ, Palmer DA, Mesmer RE (1990) Dissociation constant of bisulfate ion in aqueous sodium chloride solutions to 250°C. *J Phys Chem* 94:7978–7985
- Dickson AG, Sabine CL, Christian JR (2007) Guide to best practices for ocean CO₂ measurements. PICES Spec Publ 3, North Pacific Marine Science Organization, Sidney
- Engel A (2002) Direct relationship between CO₂-uptake and transparent exopolymer particles (TEP) production

- in natural phytoplankton. *J Plankton Res* 24:49–53
- Engel A (2009) Determination of marine gel particles. In: Wurl O (ed) Practical guidelines for the analysis of seawater. CRC Press, Boca Raton, FL, p 125–142
- Engel A, Goldthwait S, Passow U, Alldredge A (2002) Temporal decoupling of carbon and nitrogen dynamics in a mesocosm diatom bloom. *Limnol Oceanogr* 47:753–761
- Engel A, Thoms S, Riebesell U, Rochelle-Newall E, Zondervan I (2004a) Polysaccharide aggregation as a potential sink of marine dissolved organic carbon. *Nature* 428: 929–932
- Engel A, Delille B, Jacquet S, Riebesell U, Rochelle-Newall E, Terbrüggen A, Zondervan I (2004b) TEP and DOC production by *Emiliana huxleyi* exposed to different CO₂ concentrations: a mesocosm experiment. *Aquat Microb Ecol* 34:93–104
- Engel A, Zondervan I, Aerts K, Beaufort L and others (2005) Testing the direct effect of CO₂ concentration on a bloom of the coccolithophorid *Emiliana huxleyi* in mesocosm experiments. *Limnol Oceanogr* 50:493–507
- Engel A, Piontek J, Grossart HP, Riebesell U, Schulz KG, Sperling M (2014) Impact of CO₂ enrichment on organic matter dynamics during nutrient induced coastal phytoplankton blooms. *J Plankton Res*. doi:10.1093/plankt/fbt125
- Fagerbakke KM, Heldal M, Norland S (1996) Content of carbon, nitrogen, oxygen, sulfur and phosphorus in native aquatic and cultured bacteria. *Aquat Microb Ecol* 10:15–27
- Feely RA, Sabine CL, Lee K, Berelson W, Kleypas J, Fabry VJ, Millero FJ (2004) Impact of anthropogenic CO₂ on the CaCO₃ system in the oceans. *Science* 305:362–366
- Fernández E, Marañón E, Harbour DS, Kristiansen S, Heimdal BR (1996) Patterns of carbon and nitrogen uptake during blooms of *Emiliana huxleyi* in two Norwegian fjords. *J Plankton Res* 18:2349–2366
- Fichtinger-Schepman AMJ, Kamerling JP, Vliegenthart JFG, de Jong EW, Bosch L, Westbroek P (1979) Composition of a methylated, acidic polysaccharide associated with coccoliths of *Emiliana huxleyi* (Lohmann) Kamptner. *Carbohydr Res* 69:181–189
- Fiorini S, Middelburg JJ, Gattuso JP (2010) Seawater carbonate chemistry and biological processes during experiments with haploid and diploid life stages of *Emiliana huxleyi*, *Calcidiscus leptoporus* and *Syracosphaera pulchra*. *Laboratoire d'Océanographie de Villefranche*, doi:10.1594/PANGAEA.733912
- Fiorini S, Middelburg JJ, Gattuso JP (2011) Seawater carbonate chemistry, nutrients, particulate carbon and growth rate of *Emiliana huxleyi* (AC472), *Calcidiscus leptoporus* (AC370) and *Syracosphaera pulchra* (AC418) during experiments, 2011, doi:10.1594/PANGAEA.773860
- Frölicher TL, Joos F (2010) Reversible and irreversible impacts of greenhouse gas emissions in multi-century projections with the NCAR global coupled carbon cycle-climate model. *Clim Dyn* 35:1439–1459
- Gasol JM, Del Giorgio PA (2000) Using flow cytometry for counting natural planktonic bacteria and understanding the structure of planktonic bacterial communities. *Sci Mar* 64:197–224
- Gehlen M, Gangstør R, Schneider B, Bopp L, Aumont O, Ethe C (2007) The fate of pelagic CaCO₃ production in a high CO₂ ocean: a model study. *Biogeosciences* 4:505–519
- Grasshof K, Kremeling K, Ehrhardt M (1999) *Methods of seawater analysis*, 3rd edn. Wiley-VHC, Weinheim
- Harlay J, De Bodt C, Engel A, Jansen S and others (2009) Abundance and size distribution of transparent exopolymer particles (TEP) in a coccolithophorid bloom in the northern Bay of Biscay. *Deep-Sea Res* 56:1251–1265
- Hoppe CJM, Langer G, Rost B (2011) Seawater carbonate chemistry and biological processes of *Emiliana huxleyi* (strains RCC1256 and NZEH) during experiments, doi:10.1594/PANGAEA.763842
- Iglesias-Rodriguez MD, Halloran PR, Rickaby REM, Hall IR and others (2008a) Phytoplankton calcification in a high-CO₂ world. *Science* 320:336–340
- Iglesias-Rodriguez D, Halloran PR, Rickaby REM, Hall IR and others (2008b) Seawater carbonate chemistry and processes during experiments with *Emiliana huxleyi*, doi:10.1594/PANGAEA.718841
- Jannasch HW (1974) Steady state and the chemostat in ecology. *Limnol Oceanogr* 19:716–720
- Jones BM, Iglesias-Rodriguez MD, Skipp PJ, Edwards RJ and others (2013) Responses of the *Emiliana huxleyi* proteome to ocean acidification. *PLoS ONE* 8:e61868
- Kaffes A, Thoms S, Trimborn S, Rost B and others (2010) Carbon and nitrogen fluxes in the marine coccolithophore *Emiliana huxleyi* grown under different nitrate concentrations. *J Exp Mar Biol Ecol* 393:1–8
- Kleypas JA, Feely RA, Fabry VJ, Langdon C, Sabine CL, Robbins LL (2006) Impacts of ocean acidification on coral reefs and other marine calcifiers: a guide for future research. Institute for the Study of Society and Environment (ISSE) of the University Corporation for Atmospheric Research (UCAR), Boulder, CO
- Koch S (2007) Growth and calcification of the coccolithophore *Emiliana huxleyi* under different CO₂ concentrations. Diploma thesis, Institut für Chemie und Biologie des Meeres der Carl von Ossietzky Universität, Oldenburg
- Koroleff F, Grasshof K (1983) Determination of nutrients. In: Grasshof K, Erhardt M, Kremeling K (eds) *Methods of seawater analyses*. Verlag Chemie, Weinheim, p 125–188
- Langer G, Geisen M, Baumann KH, Kläs J, Riebesell U, Thoms S, Young JR (2006) Species-specific responses of calcifying algae to changing seawater carbonate chemistry. *Geochem Geophys Geosyst* 7, Q09006, doi:10.1029/2005GC001227
- Langer G, Nehrke G, Probert I, Ly J, Ziveri P (2009a) Strain-specific responses of *Emiliana huxleyi* to changing seawater carbonate chemistry. *Biogeosciences* 6:2637–2646
- Langer G, Nehrke G, Probert I, Ly J, Ziveri P (2009b) Seawater carbonate chemistry and biological processes during experiments with four strains of *Emiliana huxleyi*, doi:10.1594/PANGAEA.733946
- Langer G, Oetjen K, Brenneis T (2013) Coccolithophores do not increase particulate carbon production under nutrient limitation: a case study using *Emiliana huxleyi* (PML B92/11). *J Exp Mar Biol Ecol* 443:155–161
- LaRoche J, Rost B, Engel A (2010) Bioassays, batch culture and chemostat experimentation. In: Riebesell U, Fabry VJ, Hansson L, Gattuso J-P (eds) *Guide to best practices for ocean acidification research and data reporting*. Publications Office of the European Union, Luxembourg, p 81–94
- Lefebvre SC, Benner I, Stillman JH, Parker AE and others (2011) Seawater carbonate chemistry and carbon allocation, growth and morphology of the coccolithophore *Emiliana huxleyi* (calcifying strain CCMP 371) during experiments, doi:10.1594/PANGAEA.771910

- Leonardos N, Geider RJ (2005) Elevated atmospheric carbon dioxide increases organic carbon fixation by *Emiliana huxleyi* (Haptophyta), under nutrient-limited high-light conditions. *J Phycol* 41:1196–1203
- Lessard EJ, Merico A, Tyrrell T (2005) Nitrate: phosphate ratios and *Emiliana huxleyi* blooms. *Limnol Oceanogr* 50:1020–1024
- Lewis E, Wallace D (1998) Program developed for CO₂ system calculations. ORNL/CDIAC-105, Carbon Dioxide Information Analysis Center, Oak Ridge National Laboratory, US Department of Energy, Oak Ridge, Tennessee, http://cdiac.ornl.gov/ftp/co2sys/CO2SYS_calc_DOS_v1.05/co2sys_v1.05.txt
- Lohbeck KT, Riebesell U, Reusch TBH (2012) Adaptive evolution of a key phytoplankton species to ocean acidification. *Nat Geosci* 5:346–351
- Mantoura RFC, Llewellyn CA (1983) The rapid determination of algal chlorophyll and carotenoid pigments and their breakdown products in natural waters by reverse-phase high-performance liquid chromatography. *Anal Chim Acta* 151:297–314
- Mari X (2008) Does ocean acidification induce an upward flux of marine aggregates? *Biogeosciences Discuss* 5:1631–1654
- Matthiessen B, Eggers SL, Krug SA (2012) High nitrate to phosphorus regime attenuates negative effects of rising pCO₂ on total population carbon accumulation. *Biogeosciences* 9:1195–1203
- Mehrbach C, Culbertson CH, Hawley JE, Pytkowicz RM (1973) Measurement of apparent dissociation constants of carbonic acid in seawater at atmospheric pressure. *Limnol Oceanogr* 18:897–907
- Mucci A (1983) The solubility of calcite and aragonite in seawater at various salinities, temperature and one atmosphere total pressure. *Am J Sci* 283:780–799
- Müller M, Schulz KG, Riebesell U (2010) Seawater carbonate chemistry and processes during experiments with *Emiliana huxleyi* (2005 Bergen) and *Coccolithus braarudii* (RCC 1200), doi:10.1594/PANGAEA.744738
- Müller MN, Beaufort L, Bernard O, Pedrotti ML, Talec A, Sciandra A (2012) Influence of CO₂ and nitrogen limitation on the coccolith volume of *Emiliana huxleyi* (Haptophyta). *Biogeosciences* 9:4155–4167
- Nielsen MV (1997) Growth, dark respiration and photosynthetic parameters of the coccolithophorid *Emiliana huxleyi* (Prymnesiophyceae) acclimated to different day length-irradiance combinations. *J Phycol* 33:818–822
- Novick A, Szilard L (1950) Description of the chemostat. *Science* 112:715–716
- Obernosterer I, Herndl GJ (1995) Phytoplankton extracellular release and bacterial growth: dependence on the inorganic N:P ratio. *Mar Ecol Prog Ser* 116:247–257
- Paasche E (1998) Roles of nitrogen and phosphorus in coccolith formation in *Emiliana huxleyi* (Prymnesiophyceae). *Eur J Phycol* 33:33–42
- Paasche E (2001) A review of the coccolithophorid *Emiliana huxleyi* (Prymnesiophyceae), with particular reference to growth, coccolith formation, and calcification-photosynthesis interactions. *Phycologia* 40:503–529
- Passow U, Alldredge AL (1995) A dye-binding assay for the spectrophotometric measurement of transparent exopolymer particles (TEP) in the ocean. *Limnol Oceanogr* 40:1326–1335
- Qian J, Mopper K (1996) An automated, high performance, high temperature combustion dissolved organic carbon analyzer. *Anal Chem* 68:3090–3097
- Raven JA, Crawford K (2012) Environmental controls on coccolithophore calcification. *Mar Ecol Prog Ser* 470:137–166
- Richier S, Fiorini S, Kerros ME, von Dassow P, Gattuso JP (2011) Seawater carbonate chemistry, particulate inorganic and organic carbon and growth rate of *Emiliana huxleyi* (RCC1216) during experiments, doi:10.1594/PANGAEA.770439
- Ridgwell A, Schmidt DN, Turley C, Brownlee C, Maldonado MT, Tortell P, Young JR (2009) From laboratory manipulations to Earth system models: scaling calcification impacts of ocean acidification. *Biogeosciences* 6:2611–2623
- Riebesell U, Tortell PD (2011) Effects of acidification on pelagic organisms and ecosystems. In: Gattuso J-P, Hansson L (eds) Ocean acidification. Oxford University Press, Oxford, p 99–116
- Riebesell U, Zondervan I, Rost B, Tortell PD, Zeebe RE, Morel FMM (2000a) Reduced calcification of marine plankton in response to increased atmospheric CO₂. *Nature* 407:364–367
- Riebesell U, Zondervan I, Rost B, Tortell PD, Zeebe RE, Morel FMM (2000b) Seawater carbonate chemistry and processes during experiments with *Emiliana huxleyi* (PML B93/11A), doi:10.1594/PANGAEA.726883
- Riegman R, Stolte W, Noordeloos AAM, Slezak D (2000) Nutrient uptake and alkaline phosphatase (ec 3:1:3:1) activity of *Emiliana huxleyi* (Prymnesiophyceae) during growth under N and P limitation in continuous cultures. *J Phycol* 36:87–96
- Rokitta SD, Rost B (2012a) Effects of CO₂ and their modulation by light in the life-cycle stages of the coccolithophore *Emiliana huxleyi*. *Limnol Oceanogr* 57:607–618
- Rokitta SD, Rost B (2012b) Seawater carbonate chemistry and effects of CO₂ and their modulation by light in the life-cycle stages of the coccolithophore *Emiliana huxleyi* strains RCC 1216 and 1217 during experiments, doi:10.1594/PANGAEA.777432
- Rost B, Riebesell U, Burkhardt S, Suetemeyer D (2003) Carbon acquisition of bloom-forming marine phytoplankton. *Limnol Oceanogr* 48:55–67
- Sabine CL, Feely RA, Gruber N, Key RM and others (2004) The oceanic sink for anthropogenic CO₂. *Science* 305:367–371
- Schartau M, Engel A, Schröter J, Thoms S, Völker C, Wolf-Gladrow D (2007) Modelling carbon overconsumption and the formation of extracellular particulate organic carbon. *Biogeosciences* 4:433–454
- Sciandra A, Harlay J, Lefèvre D, Lemée R, Rimmelin P, Denis M, Gattuso JP (2003a) Response of coccolithophorid *Emiliana huxleyi* to elevated partial pressure of CO₂ under nitrogen limitation. *Mar Ecol Prog Ser* 261:111–122
- Sciandra A, Harlay J, Lefèvre D, Lemée R, Rimmelin P, Denis M, Gattuso JP (2003b) Seawater carbonate chemistry and processes during experiments with *Emiliana huxleyi* (TW1), doi:10.1594/PANGAEA.727841
- Søndergaard M, Williams PJB, Cauwet G, Riemann B and others (2000) Net accumulation and flux of dissolved organic carbon and dissolved organic nitrogen in marine plankton communities. *Limnol Oceanogr* 45:1097–1111
- Sun M, Aller RC, Lee C (1991) Early diagenesis of chlorophyll-*a* in Long Island Sound sediments: a measure of carbon flux and particle reworking. *J Mar Res* 49:379–401

- Thierstein HR, Young JR (2004) Coccolithophores: from molecular processes to global impact. Springer-Verlag, Berlin
- Toggweiler JR (1993) Carbon overconsumption. *Nature* 363: 210–211
- Tyrrell T, Merico A (2004) *Emiliana huxleyi*: bloom observations and the conditions that induce them. In: Thierstein HR, Young JR (eds) Coccolithophores: from molecular process to global impact. Springer-Verlag, Berlin, p 75–97
- Tyrrell T, Taylor AH (1996) A modelling study of *Emiliana huxleyi* in the NE Atlantic. *J Mar Syst* 9:83–112
- Van Emburg PR, de Jong EW, Daems WTh (1986) Immunohistochemical localization of a polysaccharide from biomineral structures (coccoliths) of *Emiliana huxleyi*. *J Ultrastruct Mol Struct Res* 94:246–259
- Wolf-Gladrow DA, Riebesell U, Burkhardt S, Bijma J (1999) Direct effects of CO₂ concentration on growth and isotopic composition of marine plankton. *Tellus B Chem Phys Meteorol* 51:461–476
- Zondervan I (2007) The effects of light, macronutrients, trace metals and CO₂ on the production of calcium carbonate and organic carbon in coccolithophores — a review. *Deep Sea Res II* 54:521–537
- Zondervan I, Rost B, Riebesell U (2002) Effect of CO₂ concentration on the PIC/POC ratio in the coccolithophore *Emiliana huxleyi* grown under light-limiting conditions and different daylengths. *J Exp Mar Biol Ecol* 272:55–70

*Editorial responsibility: Antonio Bode,
A Coruña, Spain*

*Submitted: September 6, 2013; Accepted: April 11, 2014
Proofs received from author(s): June 24, 2014*